

1 **Estimating Transient Climate Response in a large-ensemble global climate model simulation**

2

3 B.K. Adams and A.E. Dessler*

4 Dept. of Atmospheric Sciences, Texas A&M University, College Station, TX

5 * corresponding author, adessler@tamu.edu

6

7 Main points:

8 1. In a large model ensemble, we find that estimates of TCR from the 20th century tends to
9 be low biased compared to the model's true TCR.

10 2. Internal variability can push down or enhance the warming in ensemble members &
11 lead to large errors in TCR inferred from the 20th century.

12 3. We also verify that the details of the construction of the temperature dataset from
13 which TCR is inferred can lead to significant biases in TCR inferred from observed
14 warming.

15

16 **Plain language summary:**

17 The transient climate response (TCR) is defined to be the warming after 70 years of a 1% per
18 year increase in atmospheric CO₂. It is one of the important metrics in climate science because
19 it plays a key role in determining how much warming we will experience in the future. Previous
20 work has found that TCR inferred from observed warming over the 20th century tends to be
21 lower than TCR in climate models. This has been used by suggest that climate models are
22 overpredicting future warming. We use a large number of climate model runs to investigate
23 the methodology of this comparison. We find that TCR estimated from the 20th century
24 simulations may indeed be much lower than the model's true TCR. This arises from biases in
25 the methodology of estimating TCR from 20th century warming, as well as biases in the
26 construction of the observational temperature data sets. We therefore find no evidence that
27 models are overestimating TCR.

28

29 **Abstract**

30 The transient climate response (TCR), defined to be the warming in near-surface air
31 temperature after 70 years of a 1% per year increase in CO₂, can be estimated from observed
32 warming over the 19th and 20th centuries. Such analyses yield lower values than TCR estimated
33 from global climate models (GCMs). This disagreement has been used to suggest that GCMs'
34 climate may be too sensitive to increases in CO₂. Here we critically evaluate the methodology
35 of the comparison using a large ensemble of a fully coupled GCM simulating the historical
36 period, 1850–2005. We find that TCR estimated from model simulations of the historical period
37 can be much lower than the model's true TCR, replicating the disagreement seen between
38 observations and GCM estimates of TCR. This suggests that the disagreement could be
39 explained entirely by the details of the comparison and undercuts the suggestions that GCMs
40 overestimate TCR.

41 **Introduction**

42 The transient climate response (TCR) is frequently used to quantify the sensitivity of our climate
43 system to increases in greenhouse gases. It is defined to be the warming in near-surface air
44 temperature after 70 years of a 1% per year increase in atmospheric CO₂. As described below,
45 it can be estimated from observed warming over the 19th and 20th centuries, yielding most-
46 likely TCR values of 1.3-1.6 K [Bengtsson and Schwartz, 2013; Otto et al., 2013; Richardson et
47 al., 2016; Lewis and Curry, 2018]. These values lie below the CMIP5 ensemble average TCR of
48 1.8 K [Forster *et al.*, 2013]. This disagreement has been used to cast doubt on the fidelity of
49 model simulations of future climate change.

50 We will test the methodology of this comparison using a large model ensemble, an increasingly
51 popular tool to study the impact of internal variability on the climate system. The most
52 appropriate ensemble for this type of problem contains many runs of a single model with
53 identical physics and external forcing but different initial conditions. As each ensemble member
54 evolves in time, internal variability of the different members is out of phase, leading to
55 differences in the climate states among the ensemble members. In fact, one can think of our
56 observational record as one member of a theoretical ensemble of Earth's climate trajectories.

57 A model ensemble therefore gives us insight into what alternative climate histories may have
58 looked like.

59 **Data**

60 We analyze output from an ensemble of 100 runs of the fully-coupled Max Planck Institute
61 Earth System Model version 1.1 (MPI-ESM1.1) covering the period 1850-2005. The ensemble
62 was used by Dessler et al. [2018] to characterize the impact of internal variability on estimates
63 of the equilibrium climate sensitivity (ECS); they found that internal variability can lead to
64 significant errors in ECS inferred from historical observations. Hedemann et al. [2017] analyzed
65 this ensemble to determine potential causes of the so-called warming hiatus that occurred in
66 the 2000s.

67 This model consists of the ECHAM6.3 atmosphere and land model coupled to the MPI-OM
68 ocean model. The atmospheric resolution is T63 spectral truncation, corresponding to about
69 200 km, with 47 vertical levels, whereas the ocean has a nominal resolution of about 1.5
70 degrees and 40 vertical levels. MPI-ESM1.1 is a bug-fixed and improved version of the MPI-ESM
71 used for CMIP5 [Giorgetta *et al.*, 2013] and nearly identical to the MPI-ESM1.2 model being
72 used to provide output to CMIP6, except that the historical forcing is from the MPI-ESM. Each
73 of the 100 members simulates the years 1850-2005 and use the same evolution of historical
74 natural and anthropogenic forcings. The members differ only in their initial conditions — each
75 starts from a different state sampled from a 2000-year pre-industrial control simulation.

76 We calculate effective radiative forcing F for the ensemble by subtracting top-of-atmosphere
77 flux R in a run with climatological sea surface temperatures (SSTs) and a constant pre-industrial
78 atmosphere from average R in an ensemble of three runs using the same SSTs but the time-
79 varying atmospheric composition used in the historical runs [Hansen *et al.*, 2005; Forster *et al.*,
80 2016]. The three-member ensemble begins with perturbed atmospheric states.

81 We estimate $F_{2\times\text{CO}_2}$ using the same approach in a set of fixed SST runs, one with a pre-industrial
82 atmosphere and one in which CO_2 increases at 1% per year. We estimate $F_{2\times\text{CO}_2}$ as the average
83 difference in top-of-atmosphere flux over years 62-78, which produces a value of 3.7 W/m^2 .
84 This is lower than the value used in Dessler et al. [2018], 3.9 W/m^2 , which was estimated as

85 one-half of the average over years 130-150. We feel the value of 3.7 W/m² is a more
86 appropriate estimate of 2xCO₂ forcing in this model.

87 We will also analyze a 68-member ensemble of the MPI-ESM1.1 forced with CO₂ increasing at
88 1%/year (hereafter, “1% runs”). As with the historical ensemble, the 1% ensemble members
89 differ only in their initial conditions — each starts from a different state sampled from a 2000-
90 year pre-industrial control simulation.

91 **Analysis**

92 Time series of global-average near-surface air temperature for all 100 members are plotted in
93 Fig. 1 of Dessler et al. [2018]; that plot shows that the model ensemble is in good agreement
94 with observed surface temperatures. TCR can be estimated from the ensemble’s temperature
95 data with this equation [Gregory and Forster, 2008; Otto *et al.*, 2013; Richardson *et al.*, 2016]:

$$96 \quad \text{TCR}_{hist} = \Delta T \frac{F_{2 \times \text{CO}_2}}{\Delta F} \quad (1)$$

97 where ΔT is the change in temperature over the historical period and ΔF is the change in
98 radiative forcing. In our analysis, Δ represents the change between the 1859-1882 average,
99 selected because it is not strongly influenced by volcanic eruptions [Mauritsen and Pincus,
100 2017; Lewis and Curry, 2018], and the average of the last ten years of the runs, 1996-2005. We
101 refer to TCRs estimated this way as TCR_{hist} .

102 We first calculate TCR_{hist} in each ensemble member using global-average near-surface air
103 temperature for ΔT . The calculated values range from 1.32 to 1.94 K (5-95% range 1.48-1.90 K)
104 (Fig. 1a, Table 1). The spread in these TCR estimates is entirely due to internal variability and it
105 is similar to previous estimates [Huber *et al.*, 2014; Hawkins *et al.*, 2016]. The standard
106 deviation of ΔT from the ensemble is 0.07 K, close to that assumed by Lewis and Curry [2015],
107 implying a similar spread in TCR in their analysis.

108 TCR is formally defined as the warming of global-average near-surface air temperature in
109 response to CO₂ increasing at 1% per year, at the time of doubling (year 70). This value, which
110 we will call TCR_{true} , can be estimated by averaging the warming (relative to pre-industrial) in

111 year 70 of the 68-member ensemble of 1% runs. We find that TCR_{true} for the MPI-ESM1.1 is
112 1.81 K; this is 0.13 K (7.6%) larger than the average of the ensemble's TCR_{hist} (1.68 K).
113 Thus, TCR_{hist} is a low-biased estimate of TCR_{true} in the ensemble. The magnitude, and even the
114 sign, of this bias varies depending on the portion of the historical record being examined (Table
115 1). Overall, though, we see a clear tendency for the TCR_{hist} to underestimate TCR_{true} (Table 1).
116 Previous papers have suggested that the biases in TCR_{hist} could be due to aerosol forcing
117 efficacy [Kummer and Dessler, 2014; Shindell, 2014; Marvel *et al.*, 2015], although that
118 explanation remains to be validated in this ensemble.

119 We are now in a position to critically evaluate previous comparisons of TCR from observations
120 and GCMs. TCR estimated from observations, which are TCR_{hist} , have most-likely values in the
121 range 1.3-1.6 K [Bengtsson and Schwartz, 2013; Otto *et al.*, 2013; Richardson *et al.*, 2016; Lewis
122 and Curry, 2018], although the uncertainty in the individual estimates is large. The CMIP5
123 ensemble's TCR, which are TCR_{true} , fall in the range 1.8 ± 0.6 K (average and 5-95% confidence
124 interval) [Forster *et al.*, 2013]. Our analysis of the MPI-ESM1.1 ensemble demonstrates how a
125 model with a TCR_{true} of 1.81 K might nevertheless produce TCR_{hist} in some ensemble members
126 that that are much lower (1.3-1.4, Figure 1a) and in agreement with observational estimates.
127 Thus, differences between observational TCRs and GCM TCRs could be mostly or entirely due to
128 these issues.

129 We can also confirm previous suggestions that two issues with the observed ΔT , masking and
130 blending, are further biasing TCR_{hist} to even lower values [Richardson *et al.*, 2016]. Masking
131 refers to the fact that the observations are geographically incomplete, and that the degree of
132 incompleteness has changed over time, leading to biases in global-average ΔT [Cowtan and
133 Way, 2014]. To test the impact of this on TCR_{hist} , we also calculated ΔT in the ensemble using a
134 time-varying mask derived from HadCRUT4 (v4.6.0.0) [Morice *et al.*, 2012]. Using this masked
135 ΔT in Eq. 1, ensemble average TCR_{hist} drops from 1.68 K to 1.59 K (Fig. 1b, Table 2).

136 The second issue is blending, which refers to the fact that observed ΔT data sets are usually a
137 blend of near-surface air temperature over land and sea ice but sea surface temperature (SST)
138 over ocean. Because near-surface air temperature is warming faster than SSTs, this blending

139 lowers ΔT compared to an estimate derived entirely from near-surface air temperature [Cowtan
140 *et al.*, 2015; Santer *et al.*, 2000]. We test this by calculating a blended ΔT in the ensemble,
141 which we also mask following HadCRUT4. Using this blended and masked ΔT , ensemble
142 average TCR_{hist} drops to 1.47 K (Fig. 1d, Table 2). Importantly, none of the individual ensemble
143 members have TCR_{hist} as large as the model's TCR_{true} .

144 Finally, we have also calculated blended ΔT using the temperature of the model's top ocean
145 layer (representing the top 12 m of the ocean) instead of SST. Using that estimate of ΔT , TCR_{hist}
146 drops even further, to an ensemble average of 1.44 K (Fig. 2f, Table 2).

147 **Conclusions**

148 We have investigated why observation-based estimates of TCR tend to be lower than those
149 from GCMs. We have quantified a number of biases: 1) a bias between TCR_{hist} and TCR_{true} , 2) a
150 bias due to incomplete spatial coverage in the observational ΔT record, and 3) a bias due to the
151 observational ΔT values being blends of air temperature and SSTs. These three biases are all
152 acting in the same direction, to push TCR_{hist} to lower values. The impact of internal variability,
153 which can suppress warming in some members of the ensemble, thereby reducing TCR_{hist} , is not
154 yet quantifiable. But it has a potentially large magnitude and therefore could also be playing a
155 role in the model-observation difference.

156 The uncertainty in individual estimates of TCR_{hist} from observations are large and the range
157 easily covers most of the TCR_{true} values from the CMIP5 ensemble [Lewis and Curry, 2015; Lewis
158 and Curry, 2018; Richardson *et al.*, 2016]. Because of the large uncertainty in other parameters
159 (e.g., aerosol forcing), adding uncertainty due to the issues we discuss in this paper will produce
160 only nominal increases in the total uncertainty of the observational estimates. However, the
161 biases we have investigated are capable of explaining most or all of the disagreement between
162 the central values of the estimates, which has been the focus of much of the discussion.

163 Our work also informs how future analyses should be done. First, analyses should account for
164 the role of internal variability, most likely by comparing observations to an ensemble of runs. In
165 addition, we should not compare TCR_{hist} derived from observations to TCR_{true} — unless one can
166 quantify and adjust for the bias between these methods. A better approach would be to

167 compare TCR_{hist} from observations to TCR_{hist} derived from an ensemble of runs of the GCMs
168 covering the same period as the observations. Finally, one must account for biases in the
169 observations of ΔT due to masking and blending, most likely by calculating masked and blended
170 ΔT fields from the model and using those to estimate the model-derived TCR_{hist} .

171

172 **Acknowledgments:** This work was supported by NSF grant AGS-1661861 to Texas A&M
173 University. We thank the Bjorn Stevens, Thorsten Mauritsen, and Chris Hedemann of the Max-
174 Planck-Institut für Meteorologie for their help interpreting output from the ensemble that
175 formed the basis of this analysis. We also thank Mark Richardson for his suggestions on the
176 manuscript. Data and code are available from [insert link after paper is accepted and code is
177 finalized].

178

179 **References**

- 180 Bengtsson, L., & S. E. Schwartz (2013), Determination of a lower bound on Earth's climate
181 sensitivity, *Tellus B: Chemical and Physical Meteorology*, 65, 21533, doi:
182 10.3402/tellusb.v65i0.21533.
- 183 Cowtan, K., & R. G. Way (2014), Coverage bias in the HadCRUT4 temperature series and its
184 impact on recent temperature trends, *Q. J. R. Meteor. Soc.*, 140, 1935-1944, doi:
185 doi:10.1002/qj.2297.
- 186 Cowtan, K., Z. Hausfather, E. Hawkins, P. Jacobs, M. E. Mann, S. K. Miller, et al. (2015),
187 Robust comparison of climate models with observations using blended land air and
188 ocean sea surface temperatures, *Geophys. Res. Lett.*, 42, 6526-6534, doi:
189 10.1002/2015GL064888.
- 190 Dessler, A. E., T. Mauritsen, & B. Stevens (2018), The influence of internal variability on
191 Earth's energy balance framework and implications for estimating climate sensitivity,
192 *Atmos. Chem. Phys.*, 18, 5147-5155, doi: 10.5194/acp-18-5147-2018.
- 193 Forster, P. M., T. Andrews, P. Good, J. M. Gregory, L. S. Jackson, & M. Zelinka (2013),
194 Evaluating adjusted forcing and model spread for historical and future scenarios in the
195 CMIP5 generation of climate models, *Journal of Geophysical Research: Atmospheres*,
196 118, 1139-1150, doi: 10.1002/jgrd.50174.
- 197 Forster, P. M., T. Richardson, A. C. Maycock, C. J. Smith, B. H. Samset, G. Myhre, et al. (2016),
198 Recommendations for diagnosing effective radiative forcing from climate models for
199 CMIP6, *J. Geophys. Res.*, 121, 12460-12475, doi: 10.1002/2016jd025320.
- 200 Giorgetta, M. A., J. Jungclaus, C. H. Reick, S. Legutke, J. Bader, M. Böttinger, et al. (2013),
201 Climate and carbon cycle changes from 1850 to 2100 in MPI-ESM simulations for the

202 Coupled Model Intercomparison Project phase 5, *Journal of Advances in Modeling Earth*
203 *Systems*, 5, 572-597, doi: 10.1002/jame.20038.

204 Gregory, J. M., & P. M. Forster (2008), Transient climate response estimated from radiative
205 forcing and observed temperature change, *J. Geophys. Res.*, 113, doi:
206 10.1029/2008jd010405.

207 Hansen, J., M. Sato, R. Ruedy, L. Nazarenko, A. Lacis, G. A. Schmidt, et al. (2005), Efficacy of
208 climate forcings, *Journal of Geophysical Research: Atmospheres*, 110, doi:
209 10.1029/2005JD005776.

210 Hawkins, E., R. S. Smith, J. M. Gregory, & D. A. Stainforth (2016), Irreducible uncertainty in
211 near-term climate projections, *Climate Dynamics*, 46, 3807-3819, doi: 10.1007/s00382-
212 015-2806-8.

213 Hedemann, C., T. Mauritsen, J. Jungclaus, & J. Marotzke (2017), The subtle origins of
214 surface-warming hiatuses, *Nature Clim. Change*, 7, 336-339, doi:
215 10.1038/nclimate3274.

216 Huber, M., U. Beyerle, & R. Knutti (2014), Estimating climate sensitivity and future
217 temperature in the presence of natural climate variability, *Geophys. Res. Lett.*, 41, 2086-
218 2092, doi: 10.1002/2013GL058532.

219 Kummer, J. R., & A. E. Dessler (2014), The impact of forcing efficacy on the equilibrium
220 climate sensitivity, *Geophys. Res. Lett.*, 41, 3565-3568, doi: 10.1002/2014gl060046.

221 Lewis, N., & J. A. Curry (2015), The implications for climate sensitivity of AR5 forcing and
222 heat uptake estimates, *Climate Dynamics*, 45, 1009-1023, doi: 10.1007/s00382-014-
223 2342-y.

224 Lewis, N., & J. Curry (2018), The impact of recent forcing and ocean heat uptake data on
225 estimates of climate sensitivity, *J. Climate*, doi: 10.1175/jcli-d-17-0667.1.

226 Marvel, K., G. A. Schmidt, R. L. Miller, & L. S. Nazarenko (2015), Implications for climate
227 sensitivity from the response to individual forcings, *Nature Climate Change*, 6, 386, doi:
228 10.1038/nclimate2888.

229 Mauritsen, T., & R. Pincus (2017), Committed warming inferred from observations, *Nature*
230 *Climate Change*, 7, 652-655, doi: 10.1038/nclimate3357.

231 Morice, C. P., J. J. Kennedy, N. A. Rayner, & P. D. Jones (2012), Quantifying uncertainties in
232 global and regional temperature change using an ensemble of observational estimates:
233 The HadCRUT4 data set, *J. Geophys. Res.*, 117, doi: 10.1029/2011jd017187.

234 Otto, A., F. E. L. Otto, O. Boucher, J. Church, G. Hegerl, P. M. Forster, et al. (2013), Energy
235 budget constraints on climate response, *Nature Geoscience*, 6, 415-416, doi:
236 10.1038/ngeo1836.

237 Richardson, M., K. Cowtan, E. Hawkins, & M. B. Stolpe (2016), Reconciled climate response
238 estimates from climate models and the energy budget of Earth, *Nature Clim. Change*, 6,
239 931-935, doi: 10.1038/nclimate3066.

240 Santer, B. D., T. M. L. Wigley, D. J. Gaffen, L. Bengtsson, C. Doutriaux, J. S. Boyle, et al. (2000),
241 Interpreting differential temperature trends at the surface and in the lower
242 troposphere, *Science*, 287, 1227.

243 Shindell, D. T. (2014), Inhomogeneous forcing and transient climate sensitivity, *Nature*
244 *Climate Change*, 4, 274, doi: 10.1038/nclimate2136.

245

246

247

Table 1. TCR_{hist} calculated with different base and end periods

base period	end period	average (K)	Full TCR range (K)	5-95% TCR range (K)	width (K)	% diff from true TCR	ΔF (W/m^2)
1859-1882	1940-1949	1.82	0.63-2.88	1.15-2.50	1.35	0.4	0.54
1859-1882	1951-1960	1.96	1.10-3.13	1.32-2.67	1.34	7.6	0.59
1859-1882	1969-1978	1.71	1.01-2.91	1.24-2.24	0.99	-5.8	0.81
1859-1882	1996-2005	1.68	1.32-1.94	1.48-1.90	0.42	-7.7	1.85
1930-1939	1996-2005	1.65	0.97-2.07	1.35-1.99	0.64	-9.7	1.41
1940-1949	1996-2005	1.62	1.02-2.16	1.28-2.04	0.76	-11.5	1.31
1951-1960	1996-2005	1.55	0.91-2.04	1.20-1.90	0.70	-16.8	1.26
1970-1979	1996-2005	1.67	0.99-2.42	1.20-2.09	0.90	-8.5	0.99

248 The bold line is the case primarily discussed in the text. Width is the difference between the 5th and 95th249 percentile values; % difference is average TCR_{hist} minus TCR_{true} , 1.81 K, divided by average TCR_{hist} , in250 percent; ΔF is the change in forcing between the base and end periods.

251

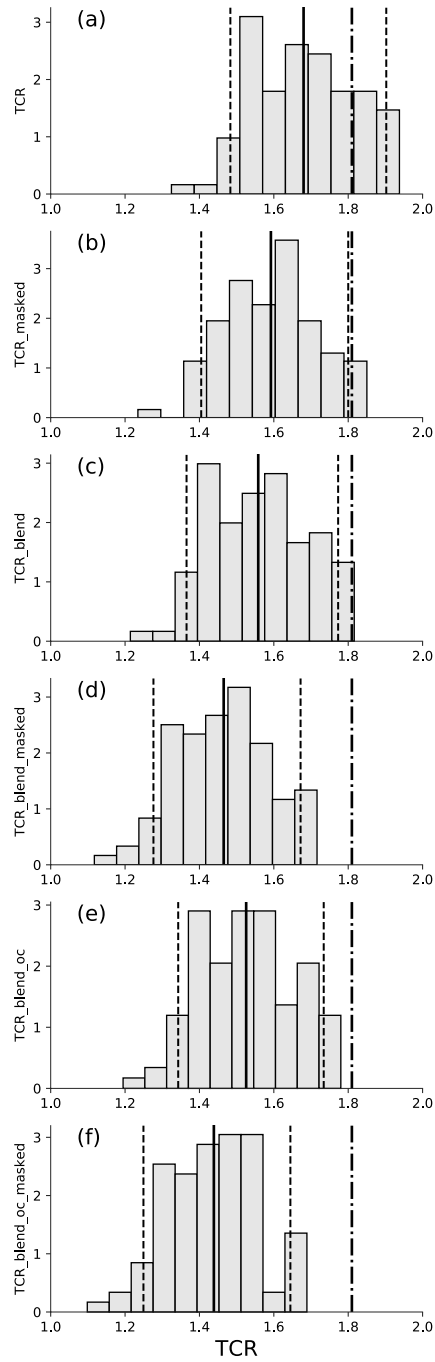
252

Table 2. TCR_{hist} calculated with different versions of ΔT

ΔT_s		average (K)	5-95% TCR range (K)	% diff from True TCR
TCR	ΔT is global-average near-surface air temperature	1.68	1.48-1.90	-7.7
TCR_masked	Same as TCR, but geographic coverage follows HadCRUT4	1.59	1.40-1.80	-13.7
TCR_blend	ΔT is a blend of near-surface air temperature over land and sea ice and SSTs over open ocean	1.56	1.37-1.77	-16.2
TCR_blend_masked	Same as TCR_blend, but geographic coverage follows HadCRUT4	1.47	1.28-1.67	-23.5
TCR_blend_oc	ΔT is a blend of near-surface air temperature over land and sea ice; elsewhere, use temperature of the top 12 m of the ocean	1.53	1.34-1.73	-18.6
TCR_blend_oc_masked	Same as TCR_blend_oc, but geographic coverage follows HadCRUT4	1.44	1.25-1.64	-25.8

253 The bold line is the base case primarily discussed in the text; % difference is average TCR_{hist} minus254 TCR_{true} , 1.81 K, divided by average TCR_{hist} , in percent.

255
256



257

258 Figure 1. Histograms of TCR_{hist} (K) from the ensemble. Each panel shows the calculation with a
259 different version of ΔT ; see Table 2 for definitions. The solid black line represents the average,
260 the dashed lines are the 5th and 95th percentiles. The dot-dashed line is TCR_{true} of the model,
261 1.81 K.